International Journal of Biochemistry and Cell Biology 113 (2019) 37–47

Contents lists available at ScienceDirect

International Journal of Biochemistry and Cell Biology

journal homepage: www.elsevier.com/locate/biocel

Resveratrol up-regulates *ATP2A3* gene expression in breast cancer cell lines through epigenetic mechanisms

Eduardo Izquierdo-Torres[a], Andrés Hernández-Oliveras[b,c], Iván Meneses-Morales[a], Gabriela Rodríguez[a], Gabriela Fuentes-García[a], Ángel Zarain-Herzberg[a,*]

[a] Departamento de Bioquímica, Facultad de Medicina. Universidad Nacional Autónoma de México, Ciudad de México, Mexico
[b] Programa de Doctorado en Ciencias de la Salud, Universidad Veracruzana, Veracruz, Mexico
[c] Instituto de Investigaciones Biológicas, Universidad Veracruzana, Xalapa, Veracruz, Mexico

ARTICLE INFO

Keywords:
SERCA
Breast cancer
Resveratrol
Epigenetics
Deacetylation
DNA methylation

ABSTRACT

Resveratrol (RSV) is a phytoestrogen which has been related to chemoprevention of several types of cancer. In this work, we show up to a 6-fold increased expression of *ATP2A3* gene induced by RSV that triggers apoptosis and changes of intracellular Ca^{2+} management in MCF-7 and MDA-MB-231 breast cancer cell lines. We explored epigenetic mechanisms for that RSV-induced *ATP2A3* up-regulation. The results indicate that RSV-induced *ATP2A3* up-regulation correlates with about 50% of reduced HDAC activity and reduced nuclear HDAC2 expression and occupancy on *ATP2A3* promoter, increasing the global acetylation of histone H3 and the enrichment of histone mark H3K27Ac on the proximal promoter of the *ATP2A3* gene in MDA-MB-231 cells. We also quantified HAT activity, finding that it can be boosted with RSV treatment; however, pharmacological inhibition of p300, one of the main HATs, did not have significant effects in RSV-mediated *ATP2A3* gene expression.

Additionally, DNMT activity was also reduced in cells treated with RSV, as well as the expression of Methyl-DNA binding proteins MeCP2 and MBD2. However, analysis of the methylation pattern of *ATP2A3* gene promoter showed un-methylated promoter in both cell lines. Taken together, the results of this work help to explain, at the molecular level, how *ATP2A3* gene is regulated in breast cancer cells, and the benefits of RSV intake observed in epidemiological data, studies with animals, and *in vitro* models.

1. Introduction

The calcium ion concentration ($[Ca^{2+}]$) functions as a second messenger which controls a wide variety of cellular processes such as differentiation, growth, and cell death, among others (Berridge et al., 2003). One of the main components of the Ca^{2+} signaling system is the Sarco/Endoplasmic Reticulum Calcium ATPase (SERCA), an enzyme which transport Ca^{2+} from the cytosol to the lumen of Endoplasmic Reticulum (ER) through ATP hydrolysis to restore the steady state (Brini and Carafoli, 2009). The SERCA pumps are encoded by three different genes (*ATP2A1-3*), whose expression is tightly regulated in tissue and development stage-specific manner (Periasamy and Kalyanasundaram, 2007). Deregulated expression of Ca^{2+} channels and pumps (including SERCA3) are characteristic features of some diseases, including breast, colon, and gastric cancer (Gelebart et al., 2002; Papp and Brouland, 2011).

Phytoestrogens are chemical compounds that are produced in plants in response to different contexts, especially stress exposure (Duffy et al., 2007). According to epidemiological studies, they have been correlated with a lower risk to develop breast cancer (Khan et al., 2012); even they have been tested in clinical studies with good outcomes, functioning as both a treatment and adjuvant therapy to minimize the side effects and resistance to chemotherapy (Cottart et al., 2014; Al Fatease et al., 2019; Jin et al., 2019; Li et al., 2017). Phytoestrogens account for multiple targets, including the epigenome (Carlos-Reyes et al., 2019). It was shown that 20–40 μM of genistein can stimulate the expression of p21 and p16, which have tumor suppression functions, such increase was correlated with inhibition of HDAC activity (Li et al., 2013); likewise, genistein and resveratrol (RSV) can reactivate the expression of Estrogen Receptor alpha (ER-α) in ER-α-negative breast cancer cells

Abbreviations: ER, Endoplasmic Reticulum; SERCA, Sarco/Endoplasmic Reticulum Ca^{2+}-ATPase Pump; RSV, Resveratrol; ER-α, Estrogen Receptor Alpha; HDAC, Histone Deacetylases; HAT, Histone Acetyltransferases

* Corresponding author at: Departamento de Bioquímica, Facultad de Medicina, Universidad Nacional Autónoma de México, Avenida Universidad 3000, Mexico City, 04510, Mexico.
E-mail address: zarain@unam.mx (Á. Zarain-Herzberg).

https://doi.org/10.1016/j.biocel.2019.05.020
Received 17 March 2019; Received in revised form 29 May 2019; Accepted 31 May 2019
Available online 04 June 2019
1357-2725/

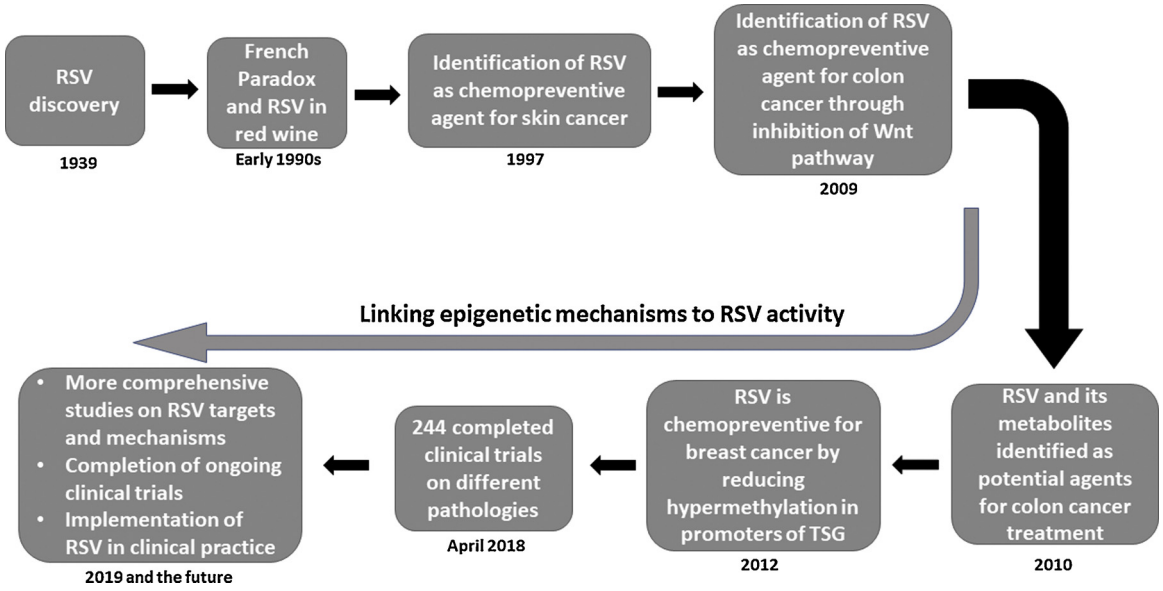

Fig. 1. Major events in the field of RSV and cancer research. RSV has been isolated from different sources, however, it was first identified in 1939 in white hellebore. In the 1990s, it was identified in red wine and suggested as a putative explanation of French Paradox, which consists in that the decreased incidence of heart disease and obesity in the French population, despite their high-fat diet, could be explained by the red wine intake in that country (Singh et al., 2019). In 1997, it was found that topical application of RSV inhibited carcinogenesis in a mouse skin cancer model (Jang et al., 1997). Colon cancer patients were treated with very small doses of RSV (< 1 mg), and Wnt signaling was inhibited in normal colonic mucosa but not in neoplastic tissue, suggesting that low doses of RSV may have a chemopreventive role for colon cancer (Nguyen et al., 2009). In 2010, patients with colorectal cancer consumed 0.5–1 g of RSV daily. RSV reached sufficient concentrations to observe pharmacologic effects, actually, it reduced cell proliferation through Ki-67 inhibition (Patel et al., 2010). In 2012, adult women with high risk to develop breast cancer consumed 10–100 mg of RSV daily for 12 weeks. High levels of RSV and metabolites were detected in serum, and methylation analysis revealed that *RASSF-1α* promoter, a Tumor Suppressor Gene (TSG) was hypomethylated compared to the women who only received placebo (Zhu et al., 2012). To April 2018, 244 clinical trials had used RSV in a broad set of pathologies (Singh et al., 2019), most of them showed beneficial effects of this molecule. As a result, more clinical and comprehensive research is needed to understand RSV mechanisms, but the data to date are promising to introduce RSV to routine clinical practice.

through the enrichment of histone marks associated with transcriptional activation on the ER-α gene promoter, due to HDAC inhibition and promotion of HAT activities (Kala and Tollefsbol, 2016). RSV also suppress the lysine methyltransferase EZH2 (Hu et al., 2019) and it is very effective to inhibit the proliferation of ER-α positive and triple negative breast cancer cells (Hu et al., 2019; Horgan et al., 2019). A time-line schematic representation of some important events in the field of RSV and cancer research are highlighted in Fig. 1.

Additionally, we previously demonstrated that RSV induces the expression of the human *ATP2A3* gene, but not of the housekeeping *ATP2A2* gene, in MCF-7 and MDA-MB-231 cells. Moreover, up-regulation of *ATP2A3* is essential for RSV-induced apoptosis in these cancer cell lines since *ATP2A3* silencing assays using siRNA partially decreases the apoptotic process induced by RSV (Izquierdo-Torres et al., 2017). Despite all the evidence, the molecular mechanisms associated with the RSV effects remain elusive. Therefore, in this work, we focus on the mechanisms for RSV-induced *ATP2A3* expression in human breast cancer cell lines, with emphasis on histone acetylation/deacetylation and CpG DNA methylation processes to shed light about how RSV works in reactivating silenced genes in the context of cancer.

2. Materials and methods

2.1. Cell cultures and treatments

MCF-7 and MDA-MB-231 breast cancer cell lines were purchased from ATCC and cultured in DMEM with high glucose + 10% FBS, 0.5% penicillin-streptomycin, and 70 mg/l kanamycin (Sigma Aldrich). Cells were grown at 37 °C in a humidified 5% CO_2/95% air atmosphere. Exponentially growing cells were trypsinized and then seeded. When cells reached 60% confluence by microscopic examination, RSV, 5-azacytidine (5-aza) or Trichostatin A (TSA) were added. Cells were treated for 72 h, replacing the culture medium every 24 h.

2.2. Cell viability assay

1×10^4 cells per well were seeded in 96-well plates. After 24 h, cells were treated with RSV (10–100 μM), TSA (50–150 nM) or 5-aza (1–5 μM). Subsequently, Prestoblue Cell Viability Reagent (1:10 in culture medium) was added, and the plate was incubated at 37 °C for 30 min. Viable cells were counted by absorbance measurements at 405 nm.

2.3. Caspases activity assay

Caspases activities were measured using the colorimetric Caspase 3 Assay Kit (Sigma-Aldrich). Briefly, 50 μg of control cells lysates and treated with RSV (10–100 μM), TSA (50–150 nM) or 5-aza (1–5 μM) were incubated for four h with the peptide substrate Ac-DEVD-pNA. The absorbance was determined at 405 nm.

2.4. RNA isolation, reverse transcription, and real-time PCR (qRT-PCR) reactions

MCF-7 and MDA-MB-231 cells were treated as described above, washed with PBS, and 1 ml of Trisure reagent (Bioline) was added to each well to isolate total RNA, according to the manufacturer's instructions. Total RNA (1 μg) was reverse-transcribed using M-MLV reverse transcriptase according to the manufacturer's instructions (Invitrogen). qRT-PCR was performed in triplicate using 50 ng of cDNA with SYBR GreenER qPCR Supermix reagent in a Rotor Gene-Q thermal cycler (Qiagen). β-actin expression was determined to normalize the results. Primer sequences are shown in Table 1.

2.5. Spectrofluorometric determination of Ca^{2+}

Control cells and treated with RSV (50 μM), 5-aza (5μM) or TSA

Table 1
Sequence of primers employed for Real-Time PCR and PCR of Bisulfite-modified DNA.

Primer name	Sequence 5'-3´	PCR Product Size (bp)
hSERCA2b	F: CGAACCCTTGCCACTCATCTTC R: TGCCGAGAACGAGCAGGATTTG	189
h-panSERCA3	F: CAGGGGACATTGTAGAAGTGGC R: TGGTCACGGACACAGATTCAC	126
hSERCA3 promoter	F: CAGATCCCACCCCTAGCAG R: TGCAGAGGGGAAACTGAGAC	116
hβ-actin	F: TGAAGGTGACAGCAGTCGGTTG R: GGCTTTTAGGATGGCAAGGGAC	146
hATP2A3 BSP	F: GGTTTAGGAGAGTTTAGAGGAG R: CCAAATACCCCAAAAA CATCC	709

F, Forward; R, Reverse.

(50 nM) were charged with 5 μM of FURA2-AM dye (Invitrogen) in Krebs buffer for 45 min at 37 °C in a humidified 5% CO_2/95% air atmosphere. Cells were then trypsinized and resuspended in Krebs Buffer pH 7.4 for monitoring fluorescence in real time at 340 nm excitation, and 510 nm of emission. Ca^{2+} release from the ER was measured by adding thapsigargin (50 μM), a specific and irreversible pan-SERCA pump inhibitor.

2.6. HDAC, HAT, and DNMT activities assays

Total HDAC and HAT activities were determined using HDAC Activity Colorimetric Assay Kit, HAT Activity Colorimetric Assay Kit Kit (Biovision), and EpiQuik DNA Methyltransferase Activity/Inhibition Assay Kit (Epigentek). 50 μg of nuclear extract from MCF-7 and MDA-MB-231 cells treated with RSV or TSA were incubated with the substrates, according to the manufacturer's instructions. Changes in absorbance were monitored during multiple time points at 405 nm (for HDAC substrate), 440 nm (for HAT substrate) or 450 nm (for 5mC).

2.7. Western blot

Fifty μg of total protein or nuclear extract from MCF-7 and MDA-MB-231 cells were separated by SDS–PAGE and transferred to a PVDF membrane (GE Healthcare Bio-Sciences). The membranes were blocked with 5% nonfat milk for two h. Primary antibodies were incubated overnight at 4 °C, and secondary antibodies were incubated 2 h at RT. Immunodetection was performed using antibodies against HDAC2, MeCP2, and MBD2/3 (Abcam), H3Ac (Millipore) and TFIIB (Santa Cruz Biotechnology) as a loading control. Detection was achieved using the chemiluminescent reactive Super Signal West Dura Extended Duration Substrate (Thermo Fisher). The luminescence of the membranes was captured in a C-Digit Blot Scanner and analyzed using the Image-Studio Lite 5.2.5 software (LI − COR).

2.8. Immunofluorescence and confocal microscopy

MCF-7 and MDA-MB-231 cells were seeded into 8-chamber culture slides (LabTek) at 5×10^4 cells/ml per chamber overnight and were treated with 50 nM TSA or 50 μM RSV. Then, cells were fixed with 1% of paraformaldehyde and permeabilized with 1% Triton X-100 followed by blockage of unspecific interaction sites with 3% BSA/PBS. After washing, the slides were incubated with the HDAC2 antibody (Abcam) overnight at 4 °C. Then, cells were incubated with Alexa Flour 488 conjugated anti-rabbit (Molecular Probes) for 2 h at RT. Later, chambers were incubated with DAPI (Sigma Aldrich) for 5 min at RT. After washing with PBS, the slides were mounted using Vectorshield® (Vector Labs). Cells were examined under a Nikon A1R + STORM confocal microscopy. Pictures were analyzed with ImageJ software.

2.9. Chromatin immunoprecipitation (ChIP) assays

MCF-7 and MDA-MB-231 cells were treated with RSV or TSA, and then they were crosslinked using 1% formaldehyde. The reaction was stopped with glycine 0.125 M. The cells were lysed and subjected to sonication in a Biorruptor Pico (Diagenode) sonication device. Immunoprecipitation was done with One-Day ChIP Kit (Diagenode) following the manufacturer instructions with some modifications. Five hundred μg of the sonicated chromatin was incubated with two μg of antibody against H3K9Ac, H3K27Ac, and HDAC2 (Abcam).

qRT-PCR quantification was performed using specific primers for the -258 to -143 bp region of the human *ATP2A3* promoter (Table 1). The data are shown as relative occupancy of the immunoprecipitated factor with respect to the negative control (anti-IgG antibody), and 10% of input DNA served as a positive control for PCR amplification.

2.10. Bisulfite-modified DNA sequencing

DNA from MCF-7 and MDA-MB-231 cells were treated with sodium bisulfite using EZ DNA Methylation-Direct Kit (Zymo Research). *ATP2A3* specific primers (Table 1) were designed using Methyl Primer Express software (Thermo Fisher Scientific) and used to carry out Bisulfite Sequencing PCR (BSP). BSP reactions were carried out with Kapa DNA polymerase (Merck) using 1 μl of bisulfite-converted genomic DNA in the Eppendorf Gradient Master Cycler, programmed with an initial incubation of 94 °C for 4 min, followed by 45 cycles of 40 s at 94 °C, 30 s at 63 °C, and 60 s at 66 °C, and a final extension step at 72 °C for 5 min. The PCR product was gel-purified and cloned using the CloneJET PCR cloning (Thermo Fisher Scientific). *Escherichia coli* DH5α cells were transformed with the ligation product, and specific primers for the plasmid were used to screen positive clones. Automated DNA sequencing analyzed the clones harboring the *ATP2A3* proximal promoter at the Molecular Biology Unit of the Instituto de Fisiología Celular, UNAM, Mexico. Sequencing data were revised with Chromas software, and methylation analysis and graphic representation were performed with BISMA software (Bisulfite Sequencing DNA Methylation Analysis).

2.11. Statistical analysis

Data were analyzed in GraphPad Prism software and are expressed as the mean of three independent experiments ± Standard Deviation (SD). Comparisons among experimental groups were made by one-way ANOVA Dunnett´s multiple comparison tests. Differences in mean values were considered significant at $p < 0.05$.

3. Results

3.1. Characterization of the effect of RSV, TSA, and 5-aza on cell viability

We compared the effect of RSV with two drugs targeting two different epigenetic mechanisms (TSA, HDACi; and 5-aza, DNMTi) on cell viability in MCF-7 and MDA-MB-231 cells. Cell viability was determined after 72 h of treatment with increasing concentrations of these drugs. We found that RSV and TSA treatments decrease cell viability in a dose-dependent manner in both cell lines. Statistically significant reduction in cell viability by RSV can be observed even at low concentrations (10 μM), using 50 μM both cell lines displayed 25% of reduction and with 100 μM it was reduced around 40–50%. Interestingly, 5-aza treatment did not have an effect on cell viability in both cell lines (Fig. 2A-B). To understand if the reduction of cell viability might be attributed to apoptosis, we measured caspases activities, finding enhanced activity in MCF-7 and MDA-MB-231 cells treated with RSV and TSA. Using 50 and 100 μM of RSV caspases activation was 2-fold compared to activation in untreated cells (Fig. 2C-D).

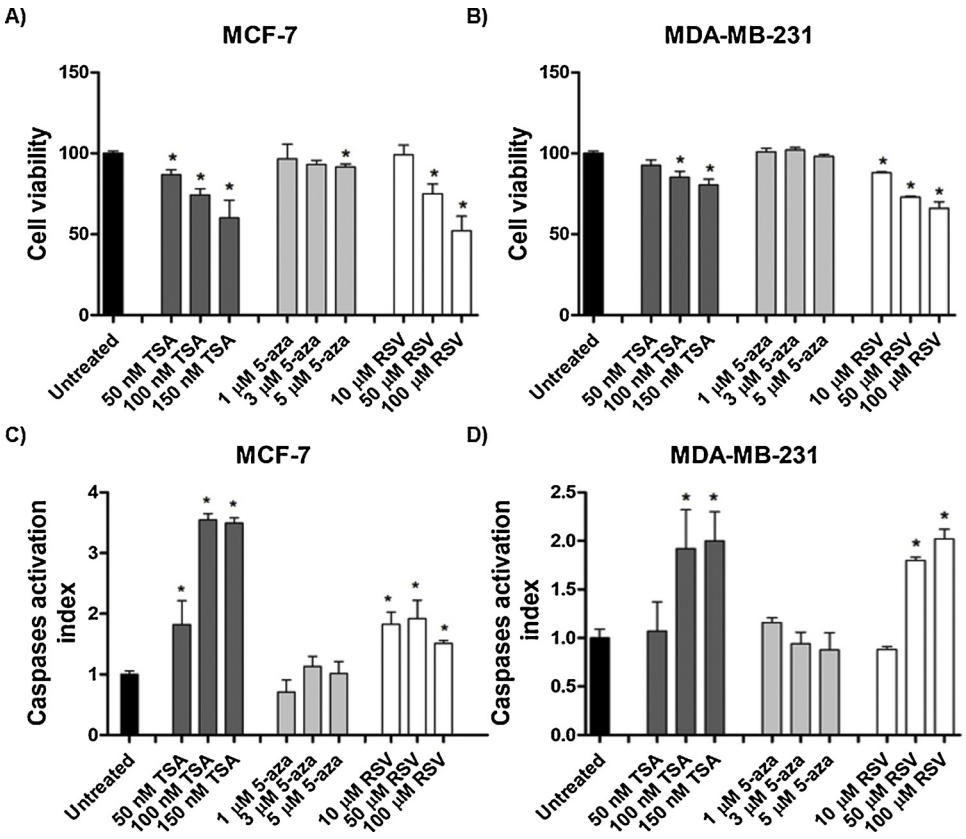

Fig. 2. RSV and TSA decrease cell viability and induce apoptosis in breast cancer cells. (A) MCF-7 and (B) MDA-MB-231 cells were treated with increasing concentrations of TSA (0–150 nM), 5-aza (1–5 μM) and RSV (0–100 μM) during 72 h, then cell viability was determined by colorimetric assays by measuring the metabolic reduction of a resazurin-based solution. (C) MCF-7 and (D) MDA-MB-231 cells were treated with increasing concentrations of TSA (0–150 nM), 5-aza (1–5 μM) or RSV (0–100 μM) during 72 h; then caspases activity was determined by colorimetric assays using the peptide substrate Ac-DEVD-pNA, which is cleaved by several caspases. Values in the figures are means ± SD of three independent experiments (N = 3). One-way ANOVA Dunnett´s multiple comparison tests, *$p < 0.05$.

3.2. The effect of RSV, TSA, and 5-aza on the expression of SERCA genes and Ca^{2+} management in breast cancer cells

When we compared the effects of RSV, TSA, and 5-aza treatments on SERCA2 and SERCA3 mRNA levels, we found that RSV elicits an increase in the relative SERCA3 mRNA level even more than TSA. RSV increased *ATP2A3* expression 2.5-fold in MCF-7 and 6-fold in MDA-MB-231 cells, whereas TSA increased 2-fold and 2.5-fold, respectively (Fig. 3A). 5-aza did not increase the SERCA3 mRNA level. The SERCA2 mRNA level was not modified by RSV, TSA, or 5-aza treatments.

We examined the effect of RSV, TSA, and 5-aza on Ca^{2+} management and found that in response to pharmacological treatments, the basal cytosolic [Ca^{2+}] and Ca^{2+} content inside the ER was different between the two cell lines. Whereas TSA and 5-aza did not trigger changes either in cytosolic [Ca^{2+}] nor in Tg-induced Ca^{2+} release in both cell lines (Fig. 3B), RSV elicited opposite effects. The basal cytosolic [Ca^{2+}] in MCF-7 cells treated with RSV was lower (111.8 nM ± 5.75) than in untreated cells (157.5 nM ± 26.5); in contrast, basal cytosolic [Ca^{2+}] in MDA-MB-231 cells treated with RSV was higher (117.6 nM ± 4.2) compared to untreated cells (49.8 nM ± 5.2) (Fig. 3B). Furthermore, Ca^{2+} release capacity from the ER was also specific for each cell line. In MCF-7 cells, RSV decreased the Tg-induced Ca^{2+} release (86.2 nM ± 9.5) compared to untreated cells (144.1 nM ± 18.2). In MDA-MB-231 cells, an opposite effect was observed, RSV increased the Tg-induced Ca^{2+} release (544.1 nM ± 21.7) compared to untreated cells (442.9.8 nM ± 14.5) (Fig. 3B).

3.3. HDAC activity, expression, and localization after RSV and TSA treatments

We compared the function of RSV and TSA as HDAC inhibitors. Therefore, we investigated the effect of TSA and RSV on HDAC class I and II activities. Both TSA and RSV inhibit HDAC class I and II activities at different extent in nuclear extracts derived from MCF-7 and MDA-MB-221 cells, albeit HDAC from MCF-7 cells are more prone to the inhibition by RSV than MDA-MB-231 cells with 71.2% *vs*. 14.1% of inhibition, respectively (Fig. 4A).

RSV has been previously proposed as a potential pan-HDAC inhibitor (Venturelli et al., 2013), although it has not been demonstrated that RSV can bind to the catalytic site of HDACs class I and II. Then, we used nuclear extract derived from untreated MCF-7 and MDA-MB-231 cells, and we added increasing concentrations of RSV (0–100 μM), finding that RSV inhibits HDAC activity in a dose-dependent manner in both cell lines (Fig. 4B). Fifty nM of TSA was used as a positive control since it is known that TSA inhibits HDACs activities by chelating a zinc ion, which is essential for their enzymatic activity (Vanhaecke et al., 2004).

Both cell lines showed an increased pattern of acetylation on histone H3 with TSA or RSV; the RSV-induced increase with RSV was 50% (Fig. 4C-E). Nevertheless, when we assessed HDAC2, we noticed that nuclear HDAC2 protein levels were reduced in nuclear extracts from MCF-7 and MDA-MB-231 cells treated with RSV (Fig. 4C-E). We also examined the subcellular localization of HDAC2 protein through immunofluorescence and confocal microscopy, finding that the nuclear localization of HDAC2 was not affected in MCF-7 and MDA-MB-231 cells when treated with RSV or TSA, although MCF-7 cells also showed cytosolic HDAC2 presence when treated with TSA and RSV (Fig. 4F-G). Analysis of HDAC2 expression in the total extract from MCF-7 and MDA-MB-231 cells showed no changes in HDAC2 expression (Fig. 4H-I).

3.4. RSV and TSA-mediated HAT activity in breast cancer cells

Histone acetyltransferases (HATs) perform the opposite activity compared to HDACs enzymes. When we measured HAT enzymatic activity in nuclear extracts, we noted that both treatments strongly increase HAT activity in MCF-7 cells (RSV by 368% and TSA by 210%), whereas the activity in MDA-MB-231 did not change significantly

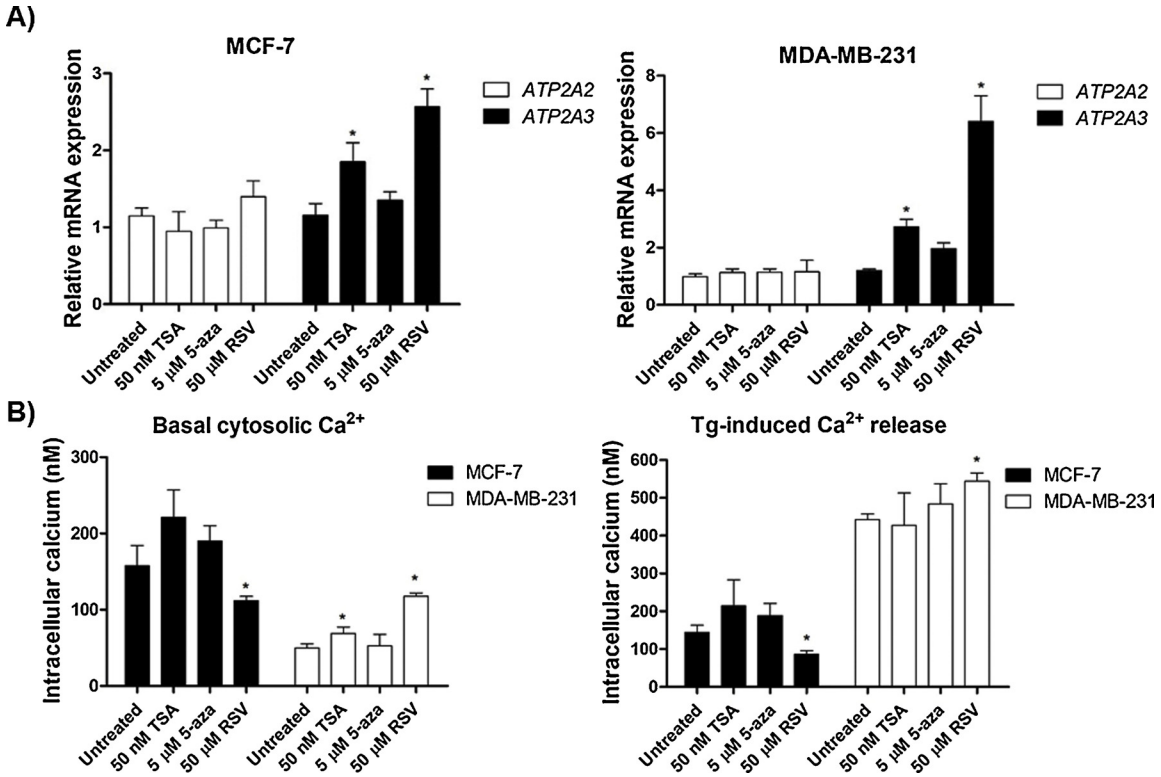

Fig. 3. RSV and TSA induce *ATP2A3* gene expression and remodeling of Ca^{2+} management in breast cancer cells. (A) MCF-7 and MDA-MB-231 cells were treated with 50 nM of TSA, 5 μM of 5-aza or 50 μM of RSV during 72 h. Then total RNA was isolated and 1 μg was retro-transcribed to determine SERCA2b and SERCA3 mRNA expression by qRT-PCR using 50 ng of cDNA. Control cells treated only with the vehicle were considered as one. (B) MCF-7 and MDA-MB-231 cells were treated with TSA (50 nM), 5-aza (5 μM) or RSV (50 μM) during 72 h; then cells were charged with FURA2-AM (5 μM) to determine Ca^{2+} concentration in basal conditions and in response to stimuli. Changes in the fluorescence were monitored in a spectrofluorometer in real time at 340 nm excitation and 510 nm emission wavelength. Ca^{2+} release from the ER was measured by adding thapsigargin (50 μM). Data are expressed as means ± SD of three independent experiments, each performed in triplicates (N = 3). One-way ANOVA Dunnett´s multiple comparison tests, *indicates values with $p < 0.05$ for experimental conditions compared to the control.

(Fig. 5A). We determined the SERCA3 mRNA expression under pharmacologically inhibited p300 activity, one of the main HATs that regulates gene transcription through chromatin remodeling. C646 is a specific p300-inhibitor (Bowers et al., 2010), and treatment of both cell lines with this compound did not alter the RSV-induced SERCA3 mRNA levels (Fig. 5B). However, when we combined C646 with RSV, SERCA3 mRNA upregulation by RSV was partially prevented in MDA-MB-231 cells (Fig. 5B).

3.5. Relative occupancy of H3K9Ac, H3K27Ac, and HDAC2 on human ATP2A3 gene promoter in breast cancer cells

We performed ChIP assays to determine the presence of acetylation-related histone marks for transcriptional activation H3K9Ac and H3K27Ac on human *ATP2A3* promoter in cells treated with RSV or TSA. The results indicate that H3K9Ac and H3K27Ac remained unchanged in MCF-7 cells treated with TSA or RSV (Fig. 6A). On the other hand, H3K9Ac also remained unchanged in MDA-MB-231 cells treated with TSA or RSV, but there is an enrichment of 78% in H3K27Ac in cells treated with TSA or RSV compared to untreated cells (Fig. 6B). Additionally, HDAC2 relative occupancy on *ATP2A3* proximal promoter decreases 63% in MDA-MB-231 cells with RSV treatment (Fig. 6C). Fig. 6D shows the acetylation and trimethylation pattern of H3K9 and H3K27 on the human *ATP2A3* gene in MCF-7 cells, according to ChIP-seq data published by the ENCODE project. It can be seen that there are ChIP-seq peaks only for H3K9Ac and H3K27Ac histone marks in the region corresponding to the *ATP2A3* promoter, while no peaks for H3K9me3 and H3K27me3 are observed.

3.6. DNMT activity and Methyl-CpG binding proteins expressed in response to RSV in breast cancer cells

Next, we analyzed the effect of RSV as a potential CpG DNA methylation inhibitor. DNMT activity in nuclear extracts obtained from MDA-MB-231 was decreased with RSV to comparable levels observed with 5-aza, 70% *vs*. 62%, respectively (Fig. 7A). On the other hand, DNMT activity in MCF-7 cells was not affected either with 5-aza nor RSV. We also analyzed the levels of the Methyl-CpG binding proteins MeCP2 and MBD2; finding that both proteins were significantly decreased in cells treated with RSV, and in smaller proportion with 5-aza (Fig. 7B-D). However, analysis of CpG methylation in *ATP2A3* gene promoter revealed that it is essentially un-methylated in MCF-7 and MDA-MB-231 cells (Fig. 7E). Interestingly, a portion of the 5´-NT region near to the translation initiation codon of the *ATP2A3* gene exon 1 was mostly methylated in MDA-MB-231 cells but un-methylated in MCF-7 cells.

4. Discussion

Aberrant gene expression is one of the earliest events in carcinogenesis, and it is involved in all hallmarks of cancer (Jones and Baylin, 2007). For this reason, it is not surprising that proteins involved in epigenetic processes and chromatin remodeling undergo mutations or alterations in their expression and function in cancer cells (Morgan and Shilatifard, 2015). The reversibility of epigenetic events makes them an attractive target for drug development, in fact some epigenetic drugs have been tested in clinical practices with good outcomes (Crump et al., 2008; Duvic et al., 2007; Richardson et al., 2008).

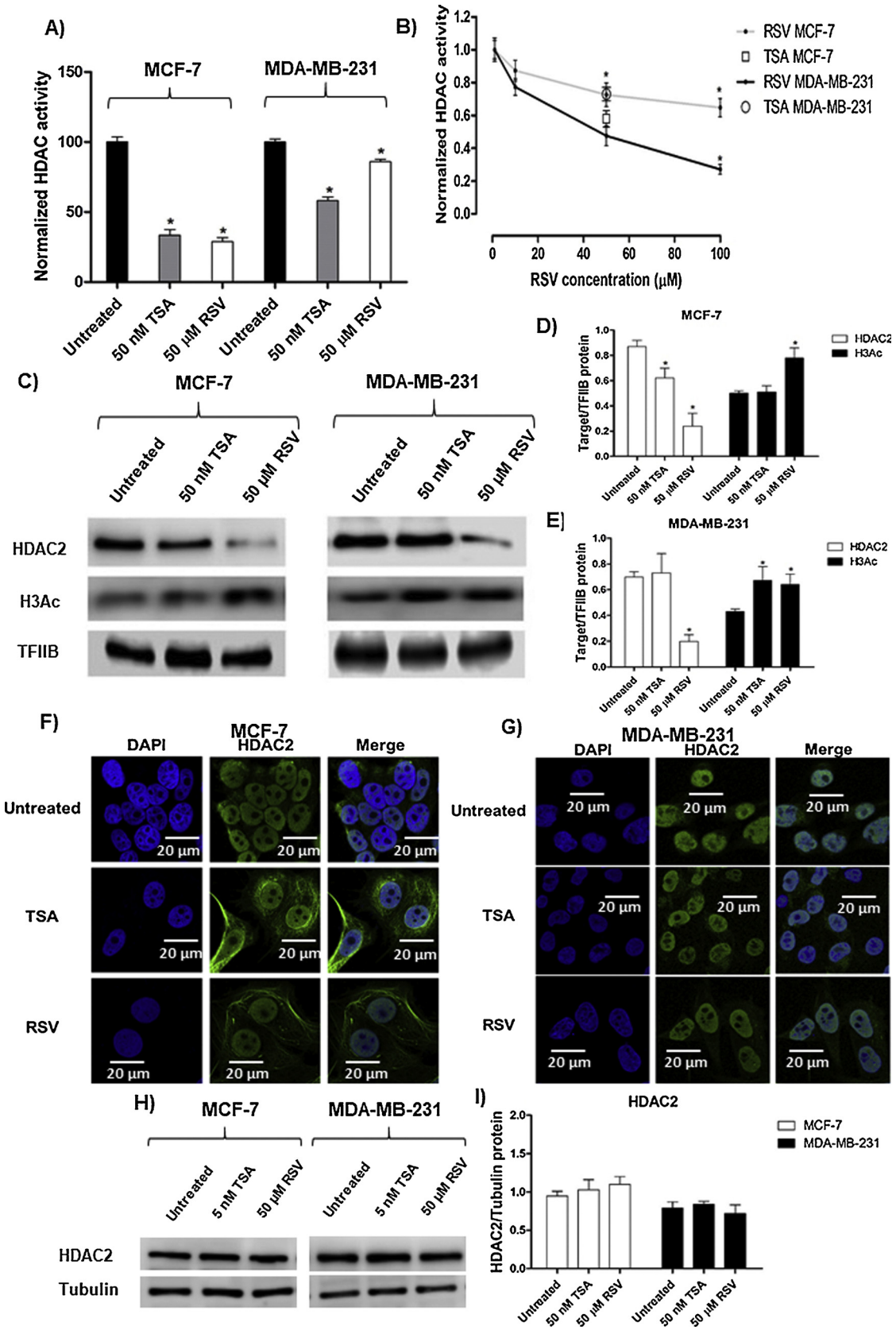

(caption on next page)

Phytoestrogens intake have been associated with a lower risk of developing several types of cancer, mainly breast cancer (Persson, 2000; Zhang et al., 2017) and has been observed as an efficient therapeutically agent against ER-α positive and triple negative breast cancer(Horgan et al., 2019; Poschner et al., 2019). It has been reviewed in the literature the role of phytoestrogens as epigenetic modulators to

Fig. 4. RSV decreases HDAC activity and nuclear HDAC2 expression, increasing total acetylation on histone H3 in breast cancer cells. (A) MCF-7 and MDA-MB-231 cells were treated with 50 nM of TSA or 50 μM of RSV during 72 h, and then nuclear extracts were isolated to determine HDAC activity using the HDAC colorimetric substrate, which comprises an acetylated lysine side chain. (B) Nuclear extracts of untreated MCF-7 and MDA-MB-231 cells were used to determine the percentage of inhibition in HDAC activity produced by increasing concentrations of RSV (0–100 μM). Values in the figures are means ± SD of three independent experiments (N = 3). HDAC2 and total H3Ac protein levels were determined by Western blot, showing (C) a representative WB image and the normalized values obtained by densitometric analysis for two independent experiments (N = 2) in (D) MCF-7 and (E) MDA-MB-231 cells. (F) MCF-7 and (G) MDA-MB-231 cells were treated with 50 nM of TSA or 50 μM of RSV during 72 h, and they were fixed with 1% of paraformaldehyde, incubated with anti-HDAC2 antibody, washed and observed by confocal microscopy. Pictures were analyzed with ImageJ software. The image is representative of two independent experiments (N = 2). Expression of total HDAC2 protein in MCF-7 and MDA-MB-231 cells, showing a representative WB image (H), and the normalized values obtained by densitometric analysis (I) for two independent experiments (N = 2). One-way ANOVA Dunnett´s multiple comparison tests, *p < 0.05.

explain the health benefits observed in several investigations (Khan et al., 2012; Carlos-Reyes et al., 2019; Singh et al., 2019). Based on the evidence that RSV had shown activity as epigenetic regulator (Kala and Tollefsbol, 2016; Venturelli et al., 2013; Mirza et al., 2013; Gao and Tollefsbol, 2018), and since we previously demonstrated that it promotes the expression of the human *ATP2A3* gene in breast cancer cells (Izquierdo-Torres et al., 2017), we decided to investigate whether *ATP2A3* up-regulation by RSV was mediated by epigenetic events, specifically histone acetylation and CpG DNA methylation.

4.1. RSV and TSA decrease cell viability and induce apoptosis in breast cancer cells

We compared the effect of RSV with two drugs targeting different epigenetic mechanisms (TSA targeting HDAC, and 5-aza targeting DNMTs). RSV and TSA decrease cell viability in a dose-dependent manner (Fig. 2A). This reduced cell viability can be attributed to apoptosis since caspases activation was detected in response to RSV and TSA in MCF-7 and MDA-MB-231 cells (Fig. 2B) as previously reported (Izquierdo-Torres et al., 2017; Kim and Bae, 2011).

4.2. RSV induces ATP2A3 gene expression in breast cancer cells and remodeling of Ca^{2+} management in breast cancer cells

We noted that RSV only up-regulates the expression of *ATP2A3* gene, whereas the housekeeping *ATP2A2* gene did never change. Based on the induction of *ATP2A3* gene (Izquierdo-Torres et al., 2017) we selected 50 μM of RSV for the remaining experiments, this concentration is within the range used in literature to study the effect of RSV on different cell targets and even is a reachable RSV blood plasma concentration after oral or intravenous administration in rats (Colom et al., 2011; Juan et al., 2010; Alayev et al., 2015; Khan et al., 2014; Qin et al., 2014).

Resveratrol enhanced SERCA3 mRNA expression in MCF-7 and MDA-MB-232 cells even more than TSA. Our data indicate that changes in the expression of SERCA genes by RSV have functional implications due to induction of apoptosis and alterations in cytosolic [Ca^{2+}] management (Figs. 2C-D and 3B). Basal cytosolic [Ca^{2+}] was lower in RSV-treated MCF-7 cells compared to untreated cells; MDA-MB-231 cells showed the opposite effect. The response to SERCA inhibition activity with thapsigargin was also different among both cell lines.

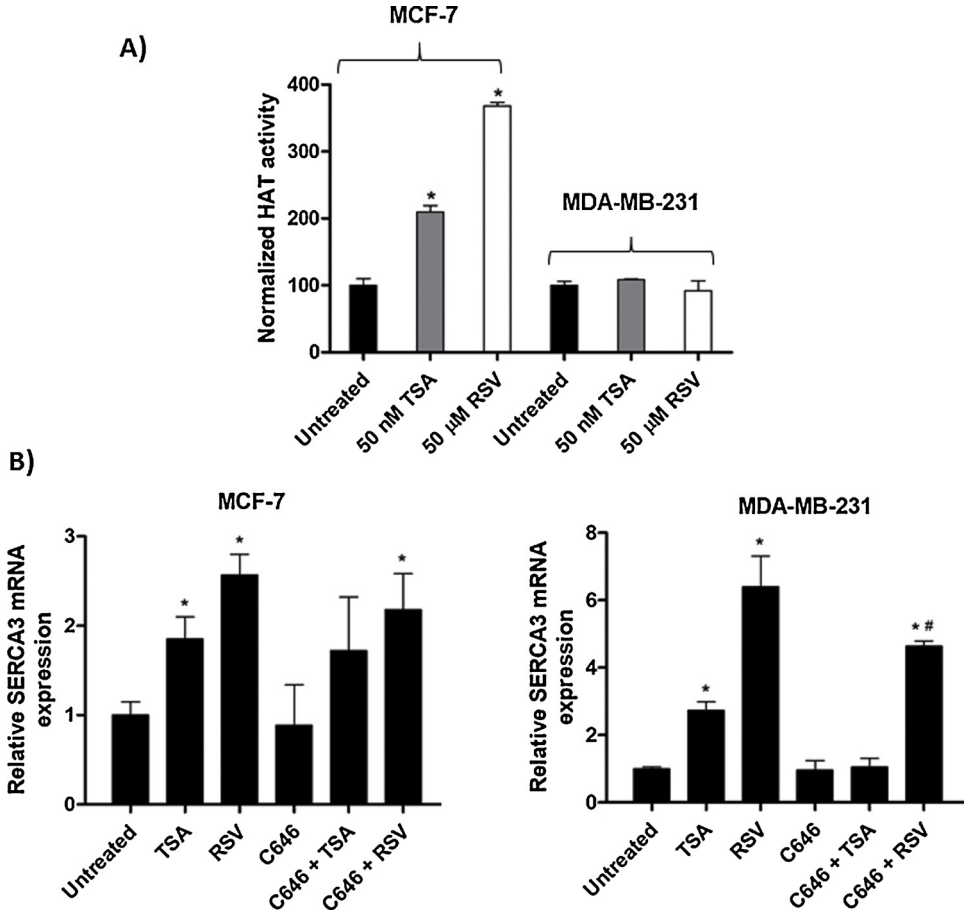

Fig. 5. RSV and TSA increased HAT activity, but combined treatment with a p300 inhibitor does not alter SERCA3 mRNA expression. (A) MCF-7 and MDA-MB-231 cells were treated with 50 nM of TSA or 50 μM of RSV during 72 h, and then nuclear extracts were isolated to determine HAT activity through spectrophotometric detection of NADH produced by CoA release due to acetylation of a peptide substrate by HATs. (B) MCF-7 and MDA-MB-231 cells were treated with 50 nM of TSA, 50 μM of RSV, 1 μM of p300-inhibitor C646, TSA + C646 or RSV-C646 during 72 h. Then total RNA was isolated and 1 μg was retrotranscribed to determine SERCA3 mRNA expression by qRT-PCR using 50 ng of cDNA. Values in the figures are means ± SD of three independent experiments (N = 3); One-way ANOVA Dunnett´s multiple comparison tests, *p < 0.05.

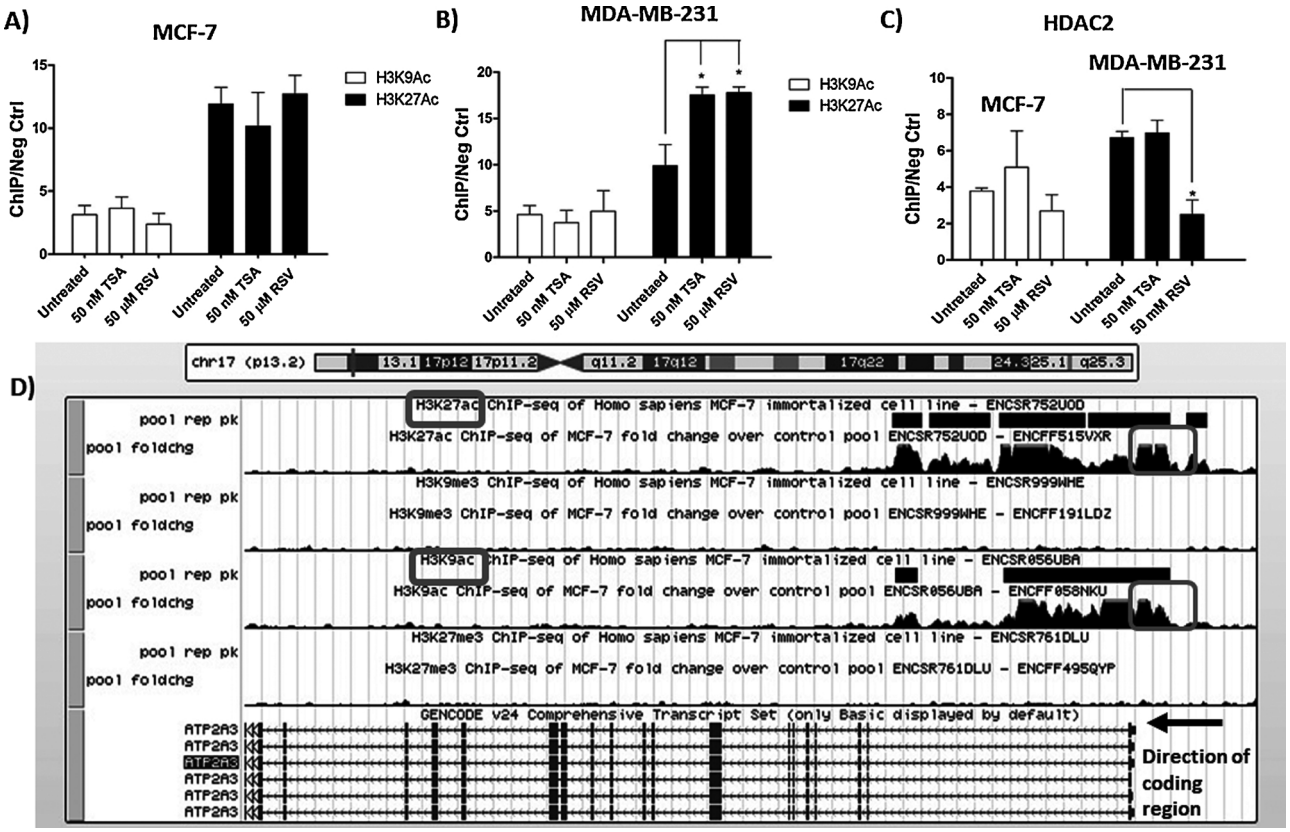

Fig. 6. RSV increases H3K27Ac and decrease HDAC2 relative occupancy on human *ATP2A3* promoter in MDA-MB-231 breast cancer cells, but not in MCF-7 cells. (A) MCF-7 and (B) MDA-MB-231 cells were treated with 50 nM of TSA or 50 μM of RSV during 72 h. Cells were crosslinked with a buffer containing 1% formaldehyde and then they were lysed, and chromatin was sheared. Chromatin Immunoprecipitation (ChIP) assays were performed using H3K9Ac, H3K27Ac and (C) HDAC2 antibodies to determine the relative occupancy of these proteins with respect to the negative control (anti-IgG antibody) on the human *ATP2A3* promoter, through qRT-PCR. A 10% input DNA served as a positive control for PCR amplification. (D) Acetylation and trimethylation pattern of H3K9 and H3K27 on the human *ATP2A3* gene in MCF-7 cells, according to ChIP-seq data published by ENCODE Project. Values in the figures are means ± SD of three independent experiments (N = 3); One-way ANOVA Dunnett´s multiple comparison tests, *$p < 0.05$.

Ca^{2+} release from ER in RSV-treated MCF-7 cells was lesser than untreated cells, whereas MDA-MB-231 cells showed the opposite effect (Fig. 3B). We suggest that the biochemical characteristics of SERCA isoforms play a key role in this phenomenon. SERCA2b has 6-times greater Ca^{2+} affinity ($_{K}Ca^{2+}$ = 0.2 μM) than SERCA3 ($_{K}Ca^{2+}$ = 1.2) (Chandrasekera et al., 2009; Dode et al., 2002). Differences in Ca^{2+} transport speed, the relative abundance of SERCA isoforms and variation in levels of other Ca^{2+} handling proteins likewise play a crucial role in Ca^{2+} homeostasis in a specific cellular context. Consequently, the prediction of Ca^{2+} variations only by analyzing the SERCA expression is challenging. Similar results were found by Gelebart et al. (2002) when compared normal KATO-III gastric cancer cells with cells treated with the HDACi butyrate. This treatment induces SERCA3 overexpression, and basal cytosolic Ca^{2+} was higher, and ER Ca^{2+} release was lower in butyrate-treated cells (Gelebart et al. (2002)).

Additionally, one of the main differences among MCF-7 and MDA-MB-231 cells is their status in ER-α expression, which is important to modulate cell behavior in breast cancer cells. Ca^{2+} and the Unfolded Protein Response (UPR) are key mediators in ER-α activation (Divekar et al., 2011; Livezey et al., 2018); this could, at least in part, explain the differences in Ca^{2+} management in these two cell lines in response to RSV and is an interesting field for upcoming research.

4.3. RSV and TSA decrease HDAC activity in breast cancer cells, but only RSV treatment decreases the abundance of nuclear HDAC2

Although RSV is considered an activator of SIRT1, sirtuins belong to the HDACs class III and differ from classical HDACs class I, II and IV in several aspects, such as structure, substrate specificity and dependence on cofactors (Haigis and Sinclair, 2010; Kupis et al., 2016), thus, it is possible that HDAC negative regulation by RSV may be through different mechanism(s). Moreover, RSV and other SIRT1 activators accelerated skin repair in a mouse model, and the same effect can be achieved by HDAC inhibitors such as TSA (Spallotta et al., 2013). Our results suggest that RSV is an HDAC inhibitor not only due to the reduction of HDAC activity (as a potentially catalytic site-mediated inhibitor) (Fig. 4A-B) but also by decreasing nuclear HDAC2 protein levels, according to our Western blot and immunofluorescence experiments (Fig. 4C-I).

4.4. RSV and TSA increase HAT activity in breast cancer cells

The RSV-mediated HDAC inhibition is enough to favor the gain of histone acetylation; nevertheless, the gain of total acetylation (Fig. 4C-E) could be stronger since RSV and TSA increased HAT activity in MCF-7 cells (Fig. 5A). These results agree with previous reports which show that RSV, pterostilbene, epigallocatechin-3-gallate (EGCG) and sulforaphane (SFN), reactivate the expression of ER-α in triple negative breast cancer cells through reversing the epigenetic aberrations that keep it silent, such as reduced HAT activity and increased HDAC and DNMT activities, neutralizing the heterochromatin context and re-sensitizing these cell lines to tamoxifen treatment (Li et al., 2017; Kala and Tollefsbol, 2016). This phenomenon was also previously observed by Kala and Tollefsbol when treated MDA-MB-157 and HCC1806 triple-negative breast cancer cells with RSV and pterostilbene to reactivate the expression of ER-α and observed decreased HDAC activity and

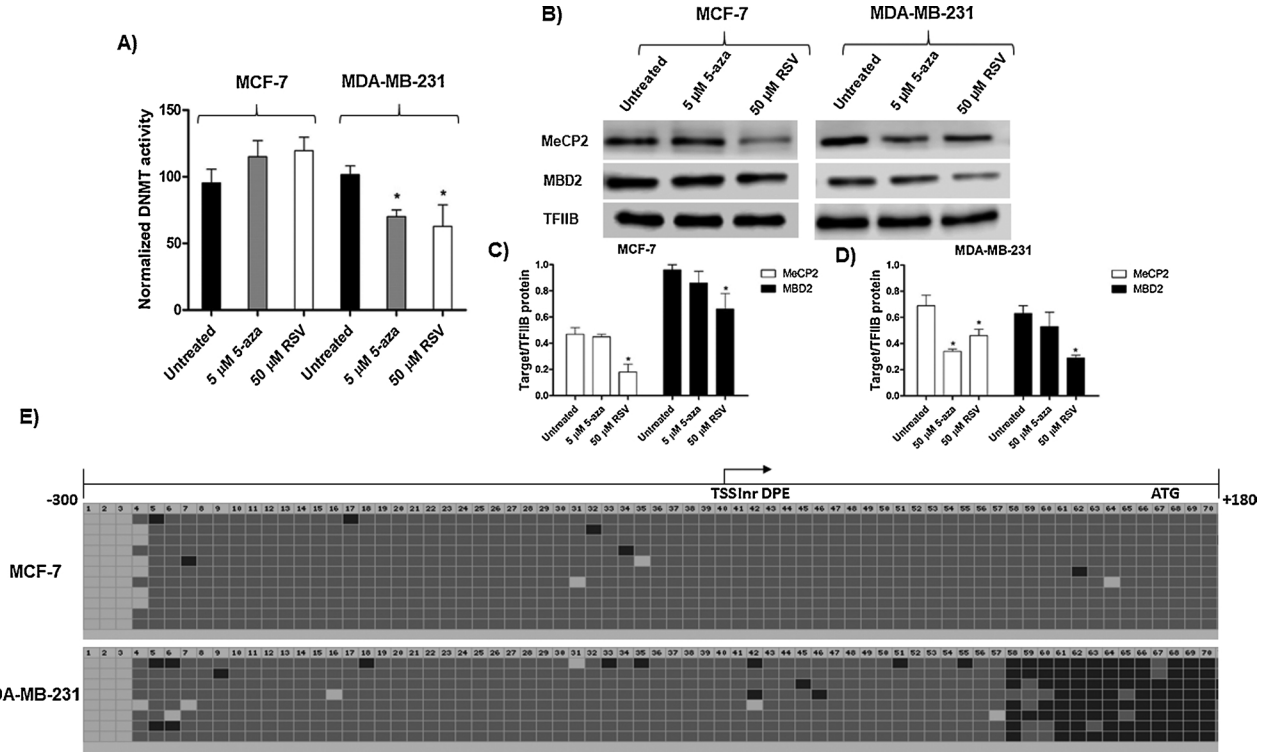

Fig. 7. RSV decreases DNMT activity and MBDs expression in breast cancer cells. (A) MCF-7 and MDA-MB-231 cells were treated with 5 μM of 5-aza or 50 μM of RSV during 72 h, and then nuclear extracts were isolated to determine DNMT activity through the methylation of a CG-rich substrate and colorimetric detection of 5mC using specific antibodies. Values in the figures are means ± SD of three independent experiments (N = 3). MeCP2 and MBD2 levels were determined by Western blot, showing (B) a representative WB image and the normalized values obtained by densitometric analysis for two independent experiments (N = 2) in (C) MCF-7, and (D) MDA-MB-231 cells. (E) MCF-7 and MDA-MB-231 cells were cultured. Genomic DNA was treated with sodium bisulfite, and *ATP2A3* promoter was amplified by PCR using methyl-specific primers. PCR product was cloned into a plasmid to transform DH5α *E. coli* cells. Plasmids containing the PCR product with *ATP2A3* promoter from both cell lines were purified and sequenced to determine the CpG methylation pattern. One-way ANOVA Dunnett´s multiple comparison tests, *$p < 0.05$.

increased HAT activity, as well as H3K9Ac enrichment on ER-α promoter (Kala and Tollefsbol, 2016).

However, when we used the p300-specific inhibitor C646, *ATP2A3* induction by RSV barely showed changes (Fig. 5B). Although we used a higher concentration (1 μM) of C646 compared to its Ki (400 nM) (Bowers et al., 2010), other studies have used 10 or 15-fold higher concentrations (Dou et al., 2018; Wang et al., 2017). Thus, it is possible that the concentration we used was not enough to prevent the RSV-mediated *ATP2A3* induction.

4.5. RSV increases H3K27Ac and decrease HDAC2 relative occupancy on ATP2A3 promoter in MDA-MB-231 breast cancer cells, but not in MCF-7 cells

The RSV-mediated activity of HDAC and HAT enzymes might create a favorable environment for transcription due to the gain of acetylation associated with transcriptional activation (Rothbart and Strahl, 2014). Accordingly, we observed an enrichment of H3K27Ac, but not H3K9Ac, on *ATP2A3* promoter in MDA-MB-231 cells treated with RSV or TSA (Fig. 6B). Surprisingly, there were no changes in levels neither on H3K9Ac nor H3K27Ac in MCF-7 cells under our experimental conditions (Fig. 6A). A possible explanation is that SERCA3 has been proposed as a differentiation marker (Flores-Peredo et al., 2017), and the cell lines used in our experiments represent different grades of differentiation. MCF-7 cells represent a luminal breast cancer subtype; in contrast, MDA-MB-231 represents a triple negative breast cancer subtype (Subik et al., 2010), which is a less differentiated and the most aggressive form of breast cancer (Hon et al., 2016). According to our results, the induction of *ATP2A3* gene by RSV is higher in MDA-MB-231 cells than in MCF-7 cells (Fig. 3A). Analysis of the threshold cycle value in real-time RT-PCR indicates that SERCA3 expression in MDA-MB-231 is much less abundant compared to MCF-7 cells under normal growing conditions, supporting the previously proposed idea that SERCA3 expression is a useful differentiation marker (Papp and Brouland, 2011). Additionally, Varga et al. 2018 demonstrated that PMCA and SERCA Ca^{2+} pumps expression is differentially regulated in a subtype specific manner when breast cancer cell lines are treated with HDACi (Varga et al., 2018).

In addition to our results, ChIP-seq data consulted from ENCODE Project show that H3K9 and H3K27 are hyperacetylated in normal conditions on *ATP2A3* promoter in MCF-7 cells (Fig. 6D), there is no data available for MDA-MB-231 cells.

RSV might also act disrupting, destabilizing or by inhibiting chromatin remodeling complexes; for instance, RSV showed the capacity to promote PTEN expression through inhibition of MTA1/HDAC complex in DU145 and PC3M prostate cancer cells (Dhar et al., 2015). Our results demonstrate that RSV treatment decrease HDAC2 occupancy on the *ATP2A3* promoter (Fig. 6C), probably inhibiting an *ATP2A3* silencing complex.

4.6. RSV decreased DNMT activity and Methyl-CpG binding proteins expression in breast cancer cells

As previously reported in MDA-MB-157 and MDA-MB-231 cells (Li et al., 2017; Kala and Tollefsbol, 2016), we confirmed a DNMT inhibition activity in response to phytoestrogens treatment (RSV), although we observed the DNMT inhibition only in MDA-MB-231 cells, whereas MCF-7 cells did not show reduced or increased DNMT activity (Fig. 7A). MeCP2 and MBD2 are proteins that usually bind methylated DNA (Bogdanovic and Veenstra, 2009). We assessed MeCP2 and MBD2

levels in the total extract from MCF-7 and MDA-MB-231 cells, finding that both proteins are reduced when cells were treated with RSV or 5-aza (Fig. 7B-D); however, the *ATP2A3* promoter in both cell lines is un-methylated (Fig. 7E). Therefore, we conclude that methylation of *ATP2A3* promoter does not play a crucial role in its RSV-induced up-regulation in breast cancer cells. Medina-Aguilar et al. analyzed the effect of RSV on the genome-wide methylation, identifying the set of genes that were hypermethylated or hypomethylated in response to RSV treatment (Medina-Aguilar et al., 2017) and *ATP2A3* was not detected, suggesting that RSV exerts its function by additional mechanisms, not only through changes in DNA methylation patterns.

4.7. Conclusions and future perspectives

In conclusion, RSV induces *ATP2A3* gene expression in MCF-7 and MDA-MB-231 breast cancer cells, triggering apoptosis, and remodeling in Ca^{2+} homeostasis. The transactivation of *ATP2A3* is correlated with reduced HDAC2 nuclear expression, reduced global HDAC activity, and enhanced global HAT activity, eliciting the enrichment of transcriptional activation histone mark H3K27Ac on *ATP2A3* promoter. DNA methylation does not play an important role in RSV-mediated *ATP2A3* up-regulation due to, although the DNTM activity was reduced, *ATP2A3* promoter is un-methylated in these cell lines. Taken together, these results contribute to the understanding of RSV-associated anticancer effect.

Although there has been intense research for years on the benefits of RSV intake on human health and disease (Fig. 1), its mechanism(s) are not fully understood. RSV and its analogs have been tested in several *in vitro* and *in vivo* studies as well as clinical trials with good outcomes (Singh et al., 2019). The complete understanding about how this and other chemopreventive agents work would give us the chance to develop more therapeutic and adjuvant options for cancer patients, consolidating the nutriepigenomics field as an important ally against cancer and other public health problems.

Funding

This work was supported by grants Dirección General de Asuntos del Personal Académico-PAPIIT-UNAMIN217216, IV200218 and IN219219 to A.Z-H. E. I-T was supported by Consejo Nacional de Ciencia y Tecnología434893 Ph.D. scholarship.

Acknowledgment

We thank Dr. Cristina Castañeda Patlán from Facultad de Medicina, UNAM and Dr. Miguel Tapia Rodríguez from Unidad de Microscopía of Instituto de Investigaciones Biomédicas, UNAM, for their technical assistance in Western blots and Confocal microscopy experiments, respectively.

References

Berridge, M.J., Bootman, M.D., Roderick, H.L., 2003. Calcium signalling: dynamics, homeostasis and remodelling. Nat. Rev. Mol. Cell Biol. 4, 517–529.
Brini, M., Carafoli, E., 2009. Calcium pumps in health and disease. Physiol. Rev. 89, 1341–1378.
Periasamy, M., Kalyanasundaram, A., 2007. SERCA pump isoforms: their role in calcium transport and disease. Muscle Nerve 35, 430–442.
Gelebart, P., Kovacs, T., Brouland, J.P., van Gorp, R., Grossmann, J., Rivard, N., Panis, Y., Martin, V., Bredoux, R., Enouf, J., Papp, B., 2002. Expression of endomembrane calcium pumps in colon and gastric cancer cells. Induction of SERCA3 expression during differentiation. J. Biol. Chem. 277, 26310–26320.
Papp, B., Brouland, J.P., 2011. Altered endoplasmic reticulum calcium pump expression during breast tumorigenesis. Breast Cancer (Auckl) 5, 163–174.
Duffy, C., Perez, K., Partridge, A., 2007. Implications of phytoestrogen intake for breast cancer. CA Cancer J. Clin. 57, 260–277.
Khan, S.I., Aumsuwan, P., Khan, I.A., Walker, L.A., Dasmahapatra, A.K., 2012. Epigenetic events associated with breast cancer and their prevention by dietary components targeting the epigenome. Chem. Res. Toxicol. 25, 61–73.
Cottart, C.H., Nivet-Antoine, V., Beaudeux, J.L., 2014. Review of recent data on the metabolism, biological effects, and toxicity of resveratrol in humans. Mol. Nutr. Food Res. 58, 7–21.
Al Fatease, A., Shah, V., Nguyen, D.X., Cote, B., LeBlanc, N., Rao, D.A., Alani, A.W., 2019. Chemosensitization and mitigation of Adriamycin-induced cardiotoxicity using combinational polymeric micelles for co-delivery of quercetin/resveratrol and resveratrol/curcumin in ovarian cancer. Nanomedicine.
Jin, X., Wei, Y., Liu, Y., Lu, X., Ding, F., Wang, J., Yang, S., 2019. Resveratrol promotes sensitization to Doxorubicin by inhibiting epithelial-mesenchymal transition and modulating SIRT1/beta-catenin signaling pathway in breast cancer. Cancer Med. 8, 1246–1257.
Li, Y., Meeran, S.M., Tollefsbol, T.O., 2017. Combinatorial bioactive botanicals re-sensitize tamoxifen treatment in ER-negative breast cancer via epigenetic reactivation of ERalpha expression. Sci. Rep. 7, 9345.
Carlos-Reyes, A., Lopez-Gonzalez, J.S., Meneses-Flores, M., Gallardo-Rincon, D., Ruiz-Garcia, E., Marchat, L.A., Astudillo-de la Vega, H., Hernandez de la Cruz, O.N., Lopez-Camarillo, C., 2019. Dietary compounds as epigenetic modulating agents in cancer. Front. Genet. 10, 79.
Li, Y., Chen, H., Hardy, T.M., Tollefsbol, T.O., 2013. Epigenetic regulation of multiple tumor-related genes leads to suppression of breast tumorigenesis by dietary genistein. PLoS One 8, e54369.
Kala, R., Tollefsbol, T.O., 2016. A novel combinatorial epigenetic therapy using resveratrol and pterostilbene for restoring estrogen receptor-alpha (ERalpha) expression in ERalpha-negative breast cancer cells. PLoS One 11, e0155057.
Hu, C., Liu, Y., Teng, M., Jiao, K., Zhen, J., Wu, M., Li, Z., 2019. Resveratrol inhibits the proliferation of estrogen receptor-positive breast cancer cells by suppressing EZH2 through the modulation of ERK1/2 signaling. Cell Biol. Toxicol.
Horgan, X.J., Tatum, H., Brannan, E., Paull, D.H., Rhodes, L.V., 2019. Resveratrol analogues surprisingly effective against triplenegative breast cancer, independent of ERalpha. Oncol. Rep. 41, 3517–3526.
Izquierdo-Torres, E., Rodriguez, G., Meneses-Morales, I., Zarain-Herzberg, A., 2017. ATP2A3 gene as an important player for resveratrol anticancer activity in breast cancer cells. Mol. Carcinog. 56, 1703–1711.
Venturelli, S., Berger, A., Bocker, A., Busch, C., Weiland, T., Noor, S., Leischner, C., Schleicher, S., Mayer, M., Weiss, T.S., Bischoff, S.C., Lauer, U.M., Bitzer, M., 2013. Resveratrol as a pan-HDAC inhibitor alters the acetylation status of histone [corrected] proteins in human-derived hepatoblastoma cells. PLoS One 8, e73097.
Vanhaecke, T., Papeleu, P., Elaut, G., Rogiers, V., 2004. Trichostatin A-like hydroxamate histone deacetylase inhibitors as therapeutic agents: toxicological point of view. Curr. Med. Chem. 11, 1629–1643.
Bowers, E.M., Yan, G., Mukherjee, C., Orry, A., Wang, L., Holbert, M.A., Crump, N.T., Hazzalin, C.A., Liszczak, G., Yuan, H., Larocca, C., Saldanha, S.A., Abagyan, R., Sun, Y., Meyers, D.J., Marmorstein, R., Mahadevan, L.C., Alani, R.M., Cole, P.A., 2010. Virtual ligand screening of the p300/CBP histone acetyltransferase: identification of a selective small molecule inhibitor. Chem. Biol. 17, 471–482.
Jones, P.A., Baylin, S.B., 2007. The epigenomics of cancer. Cell 128, 683–692.
Morgan, M.A., Shilatifard, A., 2015. Chromatin signatures of cancer. Genes Dev. 29, 238–249.
Crump, M., Coiffier, B., Jacobsen, E.D., Sun, L., Ricker, J.L., Xie, H., Frankel, S.R., Randolph, S.S., Cheson, B.D., 2008. Phase II trial of oral vorinostat (suberoylanilide hydroxamic acid) in relapsed diffuse large-B-cell lymphoma. Ann. Oncol. 19, 964–969.
Duvic, M., Talpur, R., Ni, X., Zhang, C., Hazarika, P., Kelly, C., Chiao, J.H., Reilly, J.F., Ricker, J.L., Richon, V.M., Frankel, S.R., 2007. Phase 2 trial of oral vorinostat (suberoylanilide hydroxamic acid, SAHA) for refractory cutaneous T-cell lymphoma (CTCL). Blood 109, 31–39.
Richardson, P., Mitsiades, C., Colson, K., Reilly, E., McBride, L., Chiao, J., Sun, L., Ricker, J., Rizvi, S., Oerth, C., Atkins, B., Fearen, I., Anderson, K., Siegel, D., 2008. Phase I trial of oral vorinostat (suberoylanilide hydroxamic acid, SAHA) in patients with advanced multiple myeloma. Leuk. Lymphoma 49, 502–507.
Persson, I., 2000. Estrogens in the causation of breast, endometrial and ovarian cancers - evidence and hypotheses from epidemiological findings. J. Steroid Biochem. Mol. Biol. 74, 357–364.
Zhang, Q., Feng, H., Qluwakemi, B., Wang, J., Yao, S., Cheng, G., Xu, H., Qiu, H., Zhu, L., Yuan, M., 2017. Phytoestrogens and risk of prostate cancer: an updated meta-analysis of epidemiologic studies. Int. J. Food Sci. Nutr. 68, 28–42.
Poschner, S., Maier-Salamon, A., Thalhammer, T., Jager, W., 2019. Resveratrol and other dietary polyphenols are inhibitors of estrogen metabolism in human breast cancer cells. J. Steroid Biochem. Mol. Biol. 190, 11–18.
Singh, A.P., Singh, R., Verma, S.S., Rai, V., Kaschula, C.H., Maiti, P., Gupta, S.C., 2019. Health benefits of resveratrol: evidence from clinical studies. Med. Res. Rev.
Mirza, S., Sharma, G., Parshad, R., Gupta, S.D., Pandya, P., Ralhan, R., 2013. Expression of DNA methyltransferases in breast cancer patients and to analyze the effect of natural compounds on DNA methyltransferases and associated proteins. J. Breast Cancer 16, 23–31.
Gao, Y., Tollefsbol, T.O., 2018. Combinational Proanthocyanidins and Resveratrol Synergistically Inhibit Human Breast Cancer Cells and Impact Epigenetic(-)Mediating Machinery. Int. J. Mol. Sci. 19.
Kim, H.J., Bae, S.C., 2011. Histone deacetylase inhibitors: molecular mechanisms of action and clinical trials as anti-cancer drugs. Am. J. Transl. Res. 3, 166–179.
Colom, H., Alfaras, I., Maijo, M., Juan, M.E., Planas, J.M., 2011. Population pharmacokinetic modeling of trans-resveratrol and its glucuronide and sulfate conjugates after oral and intravenous administration in rats. Pharm. Res. 28, 1606–1621.
Juan, M.E., Maijo, M., Planas, J.M., 2010. Quantification of trans-resveratrol and its metabolites in rat plasma and tissues by HPLC. J. Pharm. Biomed. Anal. 51, 391–398.
Alayev, A., Berger, S.M., Kramer, M.Y., Schwartz, N.S., Holz, M.K., 2015. The combination of rapamycin and resveratrol blocks autophagy and induces apoptosis in breast

cancer cells. J. Cell. Biochem. 116, 450–457.
Khan, A., Aljarbou, A.N., Aldebasi, Y.H., Faisal, S.M., Khan, M.A., 2014. Resveratrol suppresses the proliferation of breast cancer cells by inhibiting fatty acid synthase signaling pathway. Cancer Epidemiol. 38, 765–772.
Qin, Y., Ma, Z., Dang, X., Li, W., Ma, Q., 2014. Effect of resveratrol on proliferation and apoptosis of human pancreatic cancer MIA PaCa-2 cells may involve inhibition of the Hedgehog signaling pathway. Mol. Med. Rep. 10, 2563–2567.
Chandrasekera, P.C., Kargacin, M.E., Deans, J.P., Lytton, J., 2009. Determination of apparent calcium affinity for endogenously expressed human sarco(endo)plasmic reticulum calcium-ATPase isoform SERCA3. Am. J. Physiol., Cell Physiol. 296, C1105–1114.
Dode, L., Vilsen, B., Van Baelen, K., Wuytack, F., Clausen, J.D., Andersen, J.P., 2002. Dissection of the functional differences between sarco(endo)plasmic reticulum Ca2+-ATPase (SERCA) 1 and 3 isoforms by steady-state and transient kinetic analyses. J. Biol. Chem. 277, 45579–45591.
Divekar, S.D., Storchan, G.B., Sperle, K., Veselik, D.J., Johnson, E., Dakshanamurthy, S., Lajiminmuhip, Y.N., Nakles, R.E., Huang, L., Martin, M.B., 2011. The role of calcium in the activation of estrogen receptor-alpha. Cancer Res. 71, 1658–1668.
Livezey, M., Kim, J.E., Shapiro, D.J., 2018. A new role for estrogen receptor alpha in cell proliferation and Cancer: activating the anticipatory unfolded protein response. Front. Endocrinol. (Lausanne) 9, 325.
Haigis, M.C., Sinclair, D.A., 2010. Mammalian sirtuins: biological insights and disease relevance. Annu. Rev. Pathol. 5, 253–295.
Kupis, W., Palyga, J., Tomal, E., Niewiadomska, E., 2016. The role of sirtuins in cellular homeostasis. J. Physiol. Biochem. 72, 371–380.
Spallotta, F., Cencioni, C., Straino, S., Nanni, S., Rosati, J., Artuso, S., Manni, I., Colussi, C., Piaggio, G., Martelli, F., Valente, S., Mai, A., Capogrossi, M.C., Farsetti, A., Gaetano, C., 2013. A nitric oxide-dependent cross-talk between class I and III histone deacetylases accelerates skin repair. J. Biol. Chem. 288, 11004–11012.
Dou, C., Liu, Z., Tu, K., Zhang, H., Chen, C., Yaqoob, U., Wang, Y., Wen, J., van Deursen, J., Sicard, D., Tschumperlin, D., Zou, H., Huang, W.C., Urrutia, R., Shah, V.H., Kang, N., 2018. P300 Acetyltransferase Mediates Stiffness-Induced Activation of Hepatic Stellate Cells Into Tumor-Promoting Myofibroblasts. Gastroenterology 154, 2209–2221 e2214.
Wang, Y.M., Gu, M.L., Meng, F.S., Jiao, W.R., Zhou, X.X., Yao, H.P., Ji, F., 2017. Histone acetyltransferase p300/CBP inhibitor C646 blocks the survival and invasion pathways of gastric cancer cell lines. Int. J. Oncol. 51, 1860–1868.
Rothbart, S.B., Strahl, B.D., 2014. Interpreting the language of histone and DNA modifications. Biochim. Biophys. Acta 1839, 627–643.
Flores-Peredo, L., Rodriguez, G., Zarain-Herzberg, A., 2017. Induction of cell differentiation activates transcription of the Sarco/Endoplasmic Reticulum calcium-ATPase 3 gene (ATP2A3) in gastric and colon cancer cells. Mol. Carcinog. 56, 735–750.
Subik, K., Lee, J.F., Baxter, L., Strzepek, T., Costello, D., Crowley, P., Xing, L., Hung, M.C., Bonfiglio, T., Hicks, D.G., Tang, P., 2010. The expression patterns of ER, PR, HER2, CK5/6, EGFR, Ki-67 and AR by immunohistochemical analysis in breast Cancer cell lines. Breast Cancer (Auckl) 4, 35–41.
Hon, J.D., Singh, B., Sahin, A., Du, G., Wang, J., Wang, V.Y., Deng, F.M., Zhang, D.Y., Monaco, M.E., Lee, P., 2016. Breast cancer molecular subtypes: from TNBC to QNBC. Am. J. Cancer Res. 6, 1864–1872.
Varga, K., Hollosi, A., Paszty, K., Hegedus, L., Szakacs, G., Timar, J., Papp, B., Enyedi, A., Padanyi, R., 2018. Expression of calcium pumps is differentially regulated by histone deacetylase inhibitors and estrogen receptor alpha in breast cancer cells. BMC Cancer 18, 1029.
Dhar, S., Kumar, A., Li, K., Tzivion, G., Levenson, A.S., 2015. Resveratrol regulates PTEN/Akt pathway through inhibition of MTA1/HDAC unit of the NuRD complex in prostate cancer. Biochim. Biophys. Acta 1853, 265–275.
Bogdanovic, O., Veenstra, G.J., 2009. DNA methylation and methyl-CpG binding proteins: developmental requirements and function. Chromosoma 118, 549–565.
Medina-Aguilar, R., Perez-Plasencia, C., Gariglio, P., Marchat, L.A., Flores-Perez, A., Lopez-Camarillo, C., Garcia Mena, J., 2017. DNA methylation data for identification of epigenetic targets of resveratrol in triple negative breast cancer cells. Data Brief 11, 169–182.
Jang, M., Cai, L., Udeani, G.O., Slowing, K.V., Thomas, C.F., Beecher, C.W., Fong, H.H., Farnsworth, N.R., Kinghorn, A.D., Mehta, R.G., Moon, R.C., Pezzuto, J.M., 1997. Cancer chemopreventive activity of resveratrol, a natural product derived from grapes. Science 275, 218–220.
Nguyen, A.V., Martinez, M., Stamos, M.J., Moyer, M.P., Planutis, K., Hope, C., Holcombe, R.F., 2009. Results of a phase I pilot clinical trial examining the effect of plant-derived resveratrol and grape powder on Wnt pathway target gene expression in colonic mucosa and colon cancer. Cancer Manag. Res. 1, 25–37.
Patel, K.R., Brown, V.A., Jones, D.J., Britton, R.G., Hemingway, D., Miller, A.S., West, K.P., Booth, T.D., Perloff, M., Crowell, J.A., Brenner, D.E., Steward, W.P., Gescher, A.J., Brown, K., 2010. Clinical pharmacology of resveratrol and its metabolites in colorectal cancer patients. Cancer Res. 70, 7392–7399.
Zhu, W., Qin, W., Zhang, K., Rottinghaus, G.E., Chen, Y.C., Kliethermes, B., Sauter, E.R., 2012. Trans-resveratrol alters mammary promoter hypermethylation in women at increased risk for breast cancer. Nutr. Cancer 64, 393–400.